mathematics MDPI

Article

Generalization of Reset Controllers to Fractional Orders

Henrique Paz and Duarte Valério *

IDMEC, Instituto Superior Técnico, Universidade de Lisboa, 1049-001 Lisboa, Portugal
* Correspondence: duarte.valerio@tecnico.ulisboa.pt

Abstract: Reset control is a simple non-linear control technique that can help overcome the structural limitations of linear control. Fractional control uses the concept of fractional derivatives to expand the range of possibilities when modeling a controller, making it more robust. Fractional reset control merges the advantages of both areas and is the object of this paper. Fractional-order versions of different reset controllers were implemented, namely a fractional Clegg integrator, a fractional generalized first-order reset element, a fractional generalized second-order reset element, and fractional "constant in gain lead in phase" controllers with first- and second-order reset elements. These were computed directly from a numerical implementation of the Grünwald–Letnikov definition of fractional derivatives, and their performances were analyzed.

Keywords: fractional calculus; nonlinear control; reset control; impulsive systems

MSC: 93C27; 34A08; 93B52

check for updates

Citation: Paz, H.; Valério, D. Generalization of Reset Controllers to Fractional Orders. *Mathematics* **2022**, *10*, 4630. https://doi.org/10.3390/math10244630

Academic Editor: Christopher Goodrich

Received: 14 October 2022
Accepted: 1 December 2022
Published: 7 December 2022

1. Introduction

Linear control techniques face several limitations, as documented in [1–5], such as the trade-off between a short settling time, a low value of the overshoot or undershoot, the waterbed effect, the Bode gain–phase relation, and the design inequality that bids the achievable bandwidth of the system. Reset control is a non-linear technique that may help overcome such restrictions. It consists of resetting the output of a controller to a fraction of what it would normally be when a reset condition is triggered. Usually, this condition is a zero value at the input of the controller. Reset control was introduced in [6] and has expanded to several forms, such as in [7–9]. It allows for achieving improved phase margins while maintaining the gain behavior of its corresponding linear counterpart.

Fractional calculus introduces the concept of fractional-order derivatives and integrals. These can be used in the differential equations that synthesize controllers, opening up a way for the area of fractional control, extensively addressed in [10]. This fractional approach implies a continuous dimension of controller orders to be explored, allowing for a much wider pool of possibilities when modeling a controller's behavior. The added robustness of these controllers is documented in [10].

These two fields intersected in fractional reset control to merge the advantages of both in [11–16]. The main goal of this work is to further explore the possibilities unlocked when fractional control and reset control are combined.

The novelty of this paper is the implementation of fractional reset directly from definitions, without resorting to an integer order approximation, such as the popular CRONE approximation (introduced in [17]). In this way, it is possible to generalize reset controllers, such as the Clegg integrator (introduced in [6]), the general first-order reset element (introduced in [7]), the general second-order reset element (introduced in [9]), and the constant-gain linear phase for the previous two controllers (also introduced in [9]).

The paper is organized as follows. Section 2 addresses the concepts at the root of this work and presents an overall perspective of what was already accomplished within this particular field of study. Section 3 details the development of the synthesized fractional reset controllers and presents an application example in the simulation. Finally, Section 4 summarizes the most important conclusions to be taken from this work, states its main achievements, and points to what could be an interesting way forward.

2. Background

2.1. Fractional Calculus

Fractional calculus refers to the area of mathematics that extends the concept of $\frac{d^\alpha f(t)}{dt}$ from $\alpha = n \in \mathbb{N}$ to $\alpha \in \mathbb{R}$ or $\alpha \in \mathbb{C}$.

Functional D, which comprises both derivatives (for orders $n > 0$) and integrals (for orders $n < 0$) is introduced as

$$ {}_cD_t^n f(t) = \begin{cases} \frac{d^n f(t)}{dt^n}, & \text{if } n \in \mathbb{N} \\ f(t), & \text{if } n = 0 \\ \int_c^t {}_cD_t^{n+1} f(t)dt, & \text{if } n \in \mathbb{Z}^- \end{cases} . \tag{1} $$

Functional D can be generalized to $\mathbb{R}$ in more than one way, but here, only the Grünwald–Letnikov definition of fractional derivatives will be employed:

$$ {}_cD_t^\alpha f(t) = \lim_{h \to 0^+} \frac{\sum_{k=0}^{\lfloor \frac{t-c}{h} \rfloor} (-1)^n \binom{\alpha}{k} f(t-kh)}{h^\alpha}. \tag{2} $$

In this definition, $\alpha \in \mathbb{R}$ is the order of the fractional derivative, and combinations of a taking b at a time (also known as a choosing b) are defined as

$$ \binom{a}{b} = \begin{cases} \frac{\Gamma(a+1)}{\Gamma(b+1)\Gamma(a-b+1)}, & \text{if } a, b, a-b \in \mathbb{R} \setminus \mathbb{Z}^- \\ \frac{(-1)^b \Gamma(b-a)}{\Gamma(b+1)\Gamma(-a)}, & \text{if } a \in \mathbb{Z}^- \wedge b \in \mathbb{Z}_0^+ \\ 0, & \text{if } \left[(b \in \mathbb{Z}^- \vee b-a \in \mathbb{N}) \wedge a \notin \mathbb{Z}^-\right] \vee (a, b \in \mathbb{Z}^- \wedge |a| > |b|) \end{cases} , \tag{3} $$

resorting to the Gamma function $\Gamma(x)$:

$$ \Gamma(x) = \int_0^{+\infty} e^{-y} y^{x-1}\, \mathrm{d}y. \tag{4} $$

The reason why the Grünwald–Letnikov definition was chosen is that this definition satisfies all desirable properties that can be reasonably asked for in a fractional derivative. It reduces to (1) for integer orders, it is linear, and it generalizes the Leibniz rule and the law of exponents [18]. The Grünwald–Letnikov definition is equivalent to another definition, the Riemann–Liouville definition, for functions that are well-behaved enough, but it is more convenient from the numerical point of view [19,20]. The ease with which it can be implemented to find numerical values of fractional derivatives is used throughout this paper. For more details about the convenience of the Grünwald–Letnikov definition, see [21,22] and the references quoted above.

2.2. Reset Controllers

The reset control can be presented as an effective and simple solution among hybrid control strategies to overcome the linear design limitations addressed in [1–5]. It is a particular case of a more general type of system, called an impulsive system [23].

A reset controller is a regular controller that is equipped with a resetting mechanism that resets one or more of the controller states to zero or to a fraction of its value when a specified condition is met. The most common condition for the reset is the zero crossing of the controller's input. Reset is usually represented with an arrow crossing what is to be reset.

The set of equations defining a general reset integrator is

$$\begin{cases} \dot{u}(t) = e(t) & \text{if } c(t) \neq 0 \\ u(t^+) = a(t) & \text{if } c(t) = 0, \\ u(0) = u_0 \end{cases} \tag{5}$$

where $u(t)$ is the output of the integration of the main input $e(t)$ in flow mode (i.e., while the reset condition is not met: $c(t) \neq 0$) and resets to the after-reset value $a(t)$ in jump mode (i.e., when the reset condition $c(t_k) = 0$ is met, at the reset times $t = t_k$, $k = 1, 2, \dots$) with $u(t_k^+) = a(t_k)$. The initial condition is $u(0) = u_0$.

A state-space representation of a general reset controller with linear base dynamics would be

$$\begin{cases} \dot{\mathbf{x}}(t) = A\mathbf{x}(t) + Be(t) & \text{if } e(t) \neq 0 \\ \mathbf{x}(t^+) = A_\rho \mathbf{x}(t) & \text{if } e(t) = 0 \\ u(t) = C\mathbf{x}(t) + De(t) \\ \mathbf{x}(0) = x_0 \end{cases}, \tag{6}$$

with A, B, C, D being the state-space matrices of the base linear system, and A_ρ being the reset matrix.

The most widely studied and employed reset element in the literature, as well as the simplest, is the Clegg integrator (CI), due to its advantages which are reducing the overshoot and increasing the phase margin. The matrices for the state-space representation of the CI are

$$A = 0, \qquad B = 1, \qquad C = 1, \qquad D = 0, \qquad A_\rho = 0, \tag{7}$$

and, thus, the model becomes

$$\begin{cases} \dot{u}(t) = e(t) & \text{if } e(t) \neq 0 \\ u(t^+) = 0 & \text{if } e(t) = 0 \end{cases}. \tag{8}$$

The first-order reset element (FORE) allows for filter frequency placements, something that the CI does not; this was employed for narrowband compensation. FORE has one pole being reset.

The matrices for the state-space representation of *FORE* are

$$A = -\omega_r, \qquad B = \omega_r, \qquad C = 1, \qquad D = 0, \qquad A_\rho = 0, \tag{9}$$

resulting in model

$$\begin{cases} \dot{u}(t) = -\omega_r u(t) + \omega_r e(t) & \text{if } e(t) \neq 0 \\ u(t^+) = 0 & \text{if } e(t) = 0 \end{cases}, \tag{10}$$

where ω_r is the corner frequency.

FORE can be broadened into a generalized first-order element (GFORE), in which reset is not necessarily zero; its matrix A_γ is given by γ, the reset parameter.

Reset was applied to second-order controllers, granting one additional degree of freedom. The second-order reset element (SORE) resets its two poles.

Letting ω_r be the corner frequency and β_r the damping factor, SORE has the following state-space matrices:

$$A = \begin{bmatrix} 0 & 1 \\ -\omega_r^2 & -2\beta_r\omega_r \end{bmatrix}, \qquad B = \begin{bmatrix} 0 \\ \omega_r^2 \end{bmatrix}, \qquad C = \begin{bmatrix} 1 & 0 \end{bmatrix},$$

$$D = \begin{bmatrix} 0 \end{bmatrix}, \qquad A_\rho = \begin{bmatrix} 0 \end{bmatrix}. \tag{11}$$

Similar to what was seen for GFORE, SORE can be broadened into a generalized second-order element (GSORE).

Reset can also be employed to obtain phase lead with the "constant in gain lead in phase" (CgLp) element. The structure of CgLp consists of a reset lag filter R (which can be a GFORE or a GSORE) for broadband phase compensation in the necessary range of frequencies, in series with a linear filter L of the same order. Corner frequencies ω_r and $w_{r\eta}$ have slight shifts due to the effects of reset, and these should be tuned to match each other and obtain the most optimized frequency response.

Thus, for CgLp with GFORE, the filters are

$$R = \frac{1}{\cancelto{\gamma}{\frac{s}{w_{r\eta}} + 1}} \qquad L = \frac{\frac{s}{w_r} + 1}{\frac{s}{w_f} + 1}, \tag{12}$$

while for CgLp with GSORE, the filters are

$$R = \frac{1}{\cancelto{\gamma}{(\frac{s}{w_{r\eta}})^2 + \frac{2s\beta_r}{w_{r\eta}} + 1}} \qquad L = \frac{(\frac{s}{w_r})^2 + \frac{2s\beta_r}{w_r} + 1}{(\frac{s}{w_f})^2 + \frac{2s}{w_f} + 1}. \tag{13}$$

This results in the following state-space realization for CgLp with GFORE are:

$$A = \begin{bmatrix} -\omega_{r\eta} & 0 \\ \omega_f & -\omega_f \end{bmatrix}, \qquad B = \begin{bmatrix} \omega_{r\eta} \\ 0 \end{bmatrix}, \qquad C = \begin{bmatrix} \frac{\omega_f}{\omega_r} & \left(1 - \frac{\omega_f}{\omega_r}\right) \end{bmatrix},$$

$$D = \begin{bmatrix} 0 \end{bmatrix}, \qquad A_\rho = \begin{bmatrix} \gamma & 0 \\ 0 & 1 \end{bmatrix}, \tag{14}$$

and in the following state-space realization for CgLp with GSORE:

$$A = \begin{bmatrix} 0 & 1 & 0 & 0 \\ -\omega_{r\eta}^2 & -2\beta_r\omega_{r\eta} & 0 & 0 \\ 0 & 0 & 0 & 0 \\ 1 & 0 & -\omega_f^2 & -2\omega_f \end{bmatrix}, \qquad B = \begin{bmatrix} 0 \\ \omega_{r\eta}^2 \\ 0 \\ 0 \end{bmatrix},$$

$$C = \begin{bmatrix} \frac{\omega_f^2}{\omega_r^2} & 0 & \left(w_f^2 - \frac{\omega_f^4}{\omega_r^2}\right) & \left(\frac{2\beta_r\omega_f^2}{\omega_r} - \frac{2\omega_f^3}{\omega_r^2}\right) \end{bmatrix}, \qquad D = \begin{bmatrix} 0 \end{bmatrix}, \tag{15}$$

$$A_\rho = \begin{bmatrix} \gamma I & 0 \\ 0 & I \end{bmatrix}.$$

3. Results

The Grünwald–Letnikov definition referred to in (2) was implemented in MATLAB for a numerical vector computation. Since there is, for every machine, a limit on how large k can be in (2), this implementation doubles the sampling time where each time the limit value is reached [10].

Controllers CI, GFORE, GSORE, CgLp-GFORE, and CgLp-GSORE were also implemented in MATLAB through the state-space realizations mentioned earlier, with reset being triggered by zero-crossing of the input under a specified tolerance *tol* value and the state derivatives being integrated for each step to obtain the value of every state for the following time instant.

The responses of these controllers to input $e(t) = \sin(t)$ (including different values of parameter γ, except for CI) can be seen in Figures 1–5.

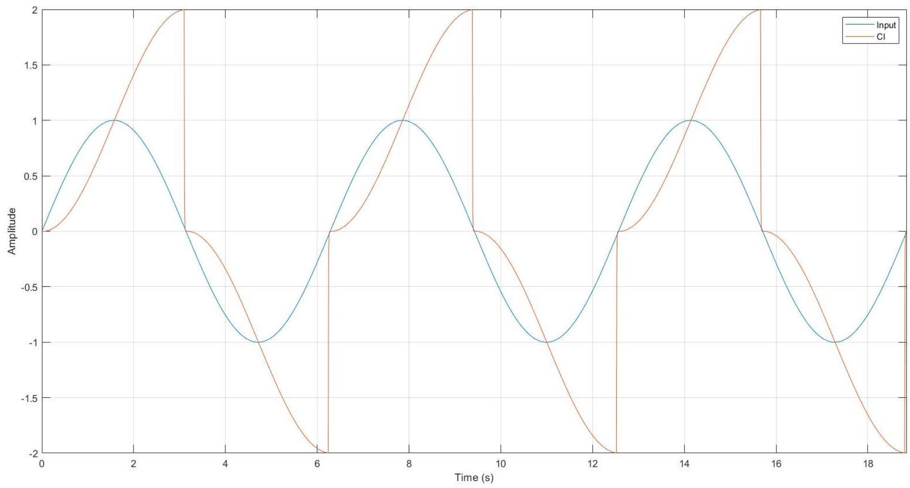

Figure 1. Response of the CI implementation to input $e(t) = \sin(t)$.

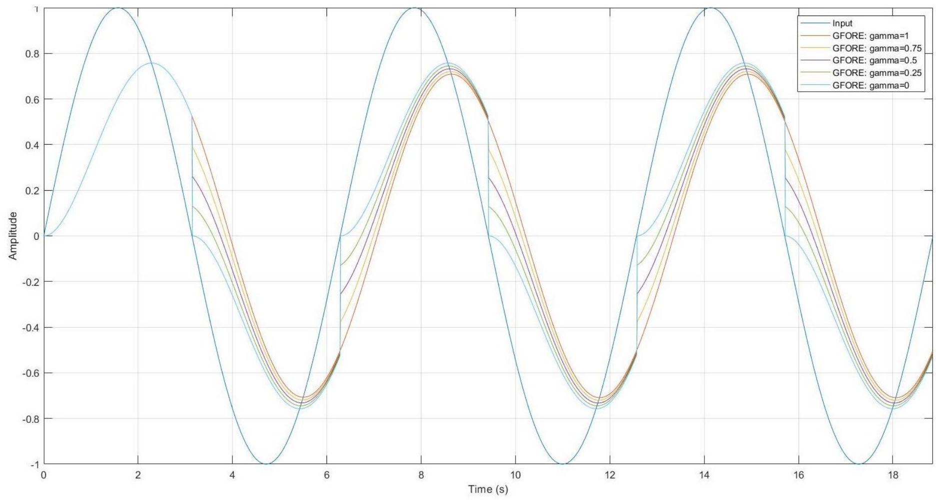

Figure 2. Response of the GFORE implementation to input $e(t) = \sin(t)$, with $\omega_r = 1$, and different values of γ.

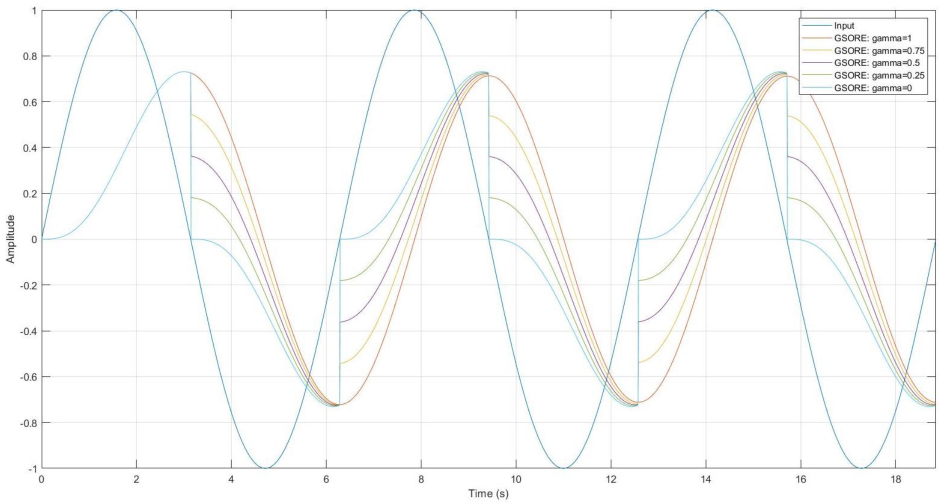

Figure 3. Response of the GSORE implementation to input $e(t) = \sin(t)$, with $\omega_r = 1$, $\beta = \frac{\sqrt{2}}{2}$ and different values of γ.

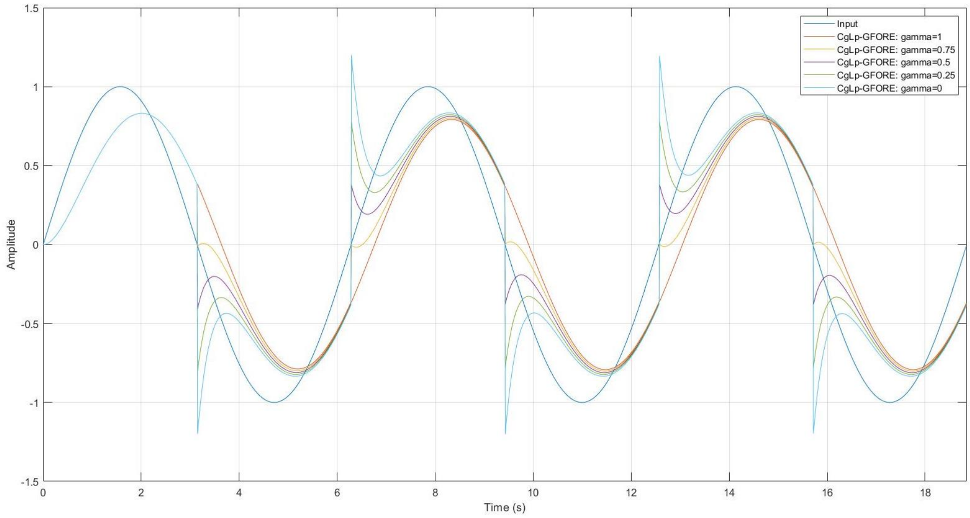

Figure 4. Response of the CgLp-GFORE implementation to input $e(t) = \sin(t)$, with $\omega_r = 1$, $\omega_\eta = 0.73$, $\omega_f = 3$ and different values of γ.

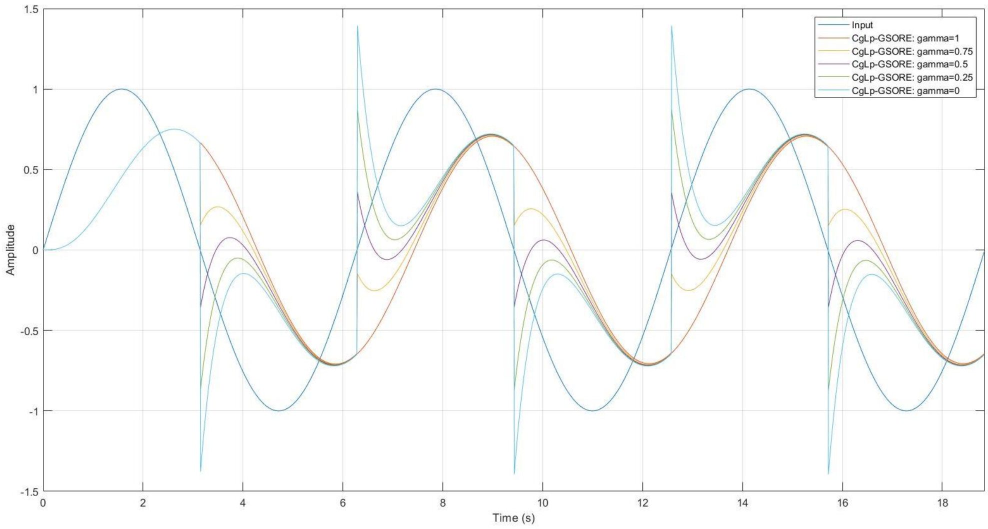

Figure 5. Response of the CgLp-GSORE implementation to input $e(t) = \sin(t)$, with $\omega_r = 1$, $\omega_\eta = 0.95$, $\omega_f = 1.7$, $\beta = \frac{\sqrt{2}}{2}$ and different values of γ.

Notice that, for CgLp-GFORE and CgLp-GSORE, lower values of γ may lead the responses to have significantly higher overshoots, while the effect of γ is the opposite for the other controllers.

3.1. Generalization to Fractional Orders

These controllers were generalized to fractional orders through the Grünwald–Letnikov implementation of the fractional derivative. The numerical strategy employed was as follows:

- We calculated a fractional derivative with an order λ, such that the obtained quantity became the integrable slope of the desired fractional derivative of order α (e.g., for a fractional CI, $\lambda = \alpha + 1$);
- We integrated the result at each time step (thus, for the fractional CI, the order became $\lambda + (-1) = \alpha$);
- At the reset instances, the integration result was multiplied by γ.

Both responses to a sinusoidal input (similar to those in Figures 1–5) and the describing function method were employed to analyze the frequency domain behavior of each controller and assess if the desired behavior was attained.

3.2. Fractional CI

The fractional implementation of CI includes the option of a partial reset; its transfer function is

$$G_c = \cancelto{\gamma}{s^{\alpha}}. \tag{16}$$

Responses to input $e(t) = \sin(t)$ for different values of parameters α and γ are given in Figures 6 and 7. The corresponding describing functions can be seen in Figures 8 and 9 for different orders of parameters α and γ.

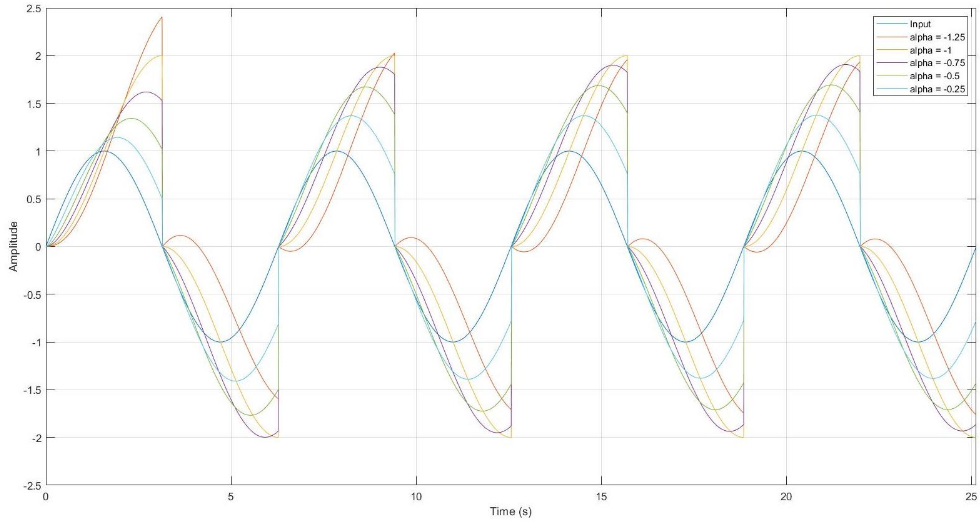

Figure 6. Response of the fractional Clegg integrator to input $e(t) = \sin(t)$, with $\gamma = 0$, and different values of α.

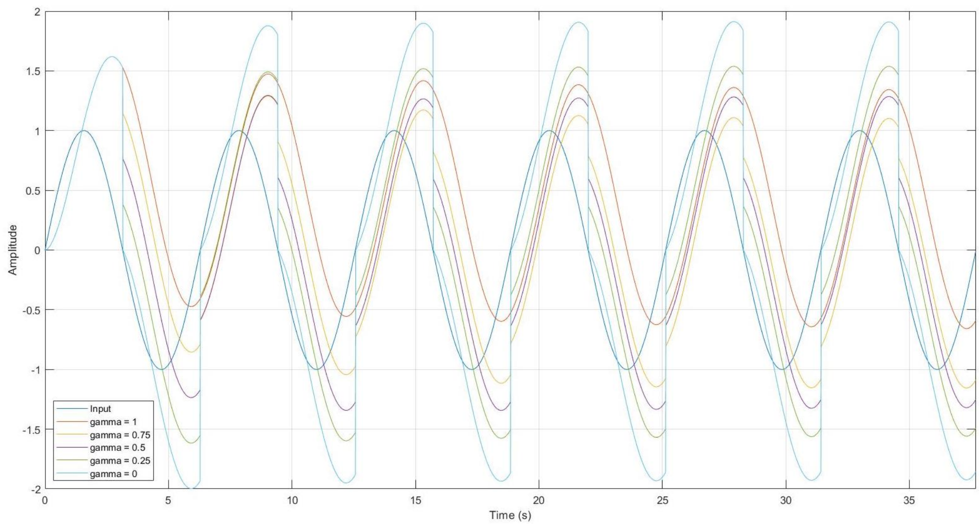

Figure 7. Response of the fractional Clegg integrator to input $e(t) = \sin(t)$, with $\alpha = -0.75$, and different values of γ.

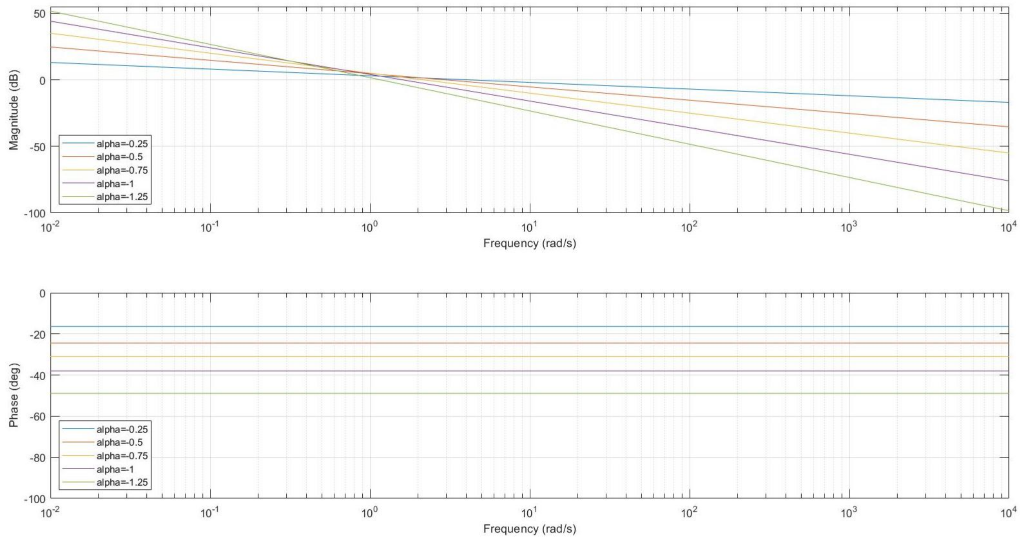

Figure 8. Describing function for the fractional Clegg integrator (second implementation), with $\gamma = 0$ for several orders of α.

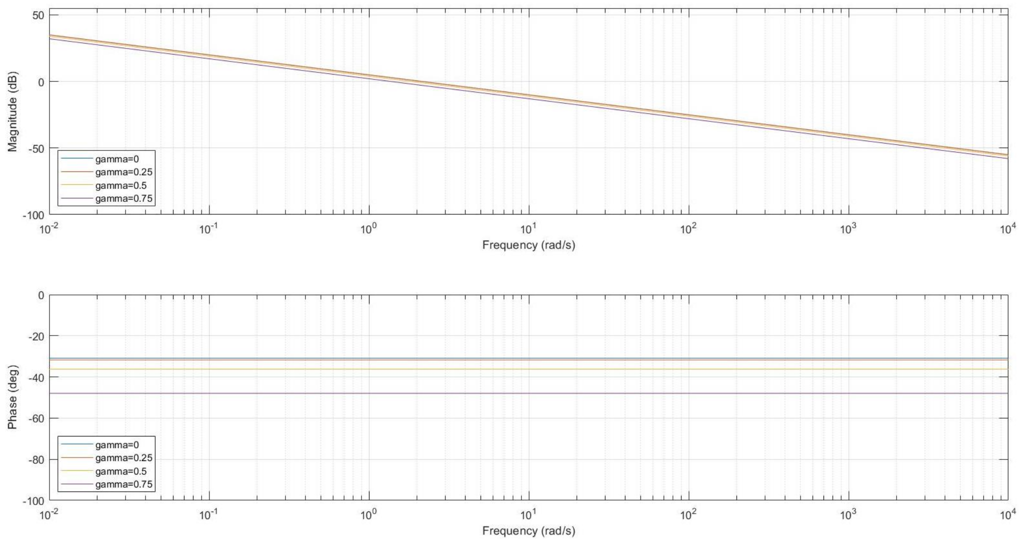

Figure 9. Describing function for the fractional Clegg integrator (second implementation), with $\alpha = -0.75$ for several orders of γ.

3.3. Fractional GFORE

The fractional generalization of GFORE, the generalized fractional-order reset element (GFrORE), has the following transfer function:

$$G_c = \frac{\omega_r}{s^{\alpha} + \omega_r};\gamma \tag{17}$$

The differential equation that relates the controller input $e(t)$ to the controller output $u(t)$, without making the reset explicit, is, for this controller,

$$u(t) = e(t) - \frac{1}{\omega_r} D^{\alpha} u(t), \tag{18}$$

$$D^{\alpha} u(t) = \omega_r e(t) - \omega_r u(t). \tag{19}$$

In order to obtain the integrable slope of $u(t)$, the expression for the first-order derivative of $u(t)$ is obtained:

$$D^{\lambda} D^{\alpha} u(t) = D^{\lambda}(\omega_r e(t) - \omega_r u(t)), \tag{20}$$

$$\lambda + \alpha = 1, \tag{21}$$

$$D^{1} u(t) = D^{1-\alpha}(\omega_r e(t) - \omega_r u(t)). \tag{22}$$

This implementation allows employing the step-by-step integration already used in other implementations. Responses to the input $e(t) = \sin(t)$ for different values of parameters α and γ can be seen in Figures 10 and 11. The describing functions are given in Figures 12 and 13.

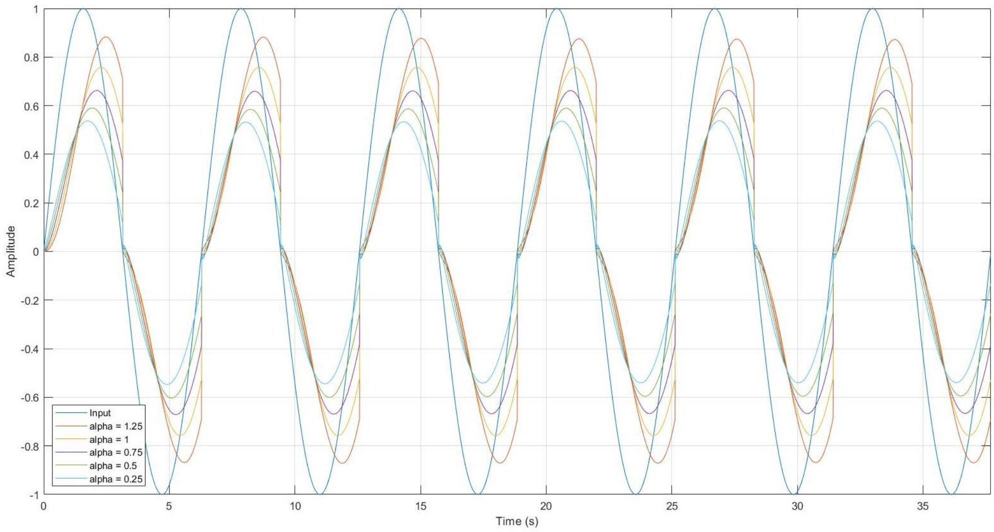

Figure 10. Response of the fractional GFORE to input $e(t) = \sin(t)$, with $\omega_r = 1$, $\gamma = 0$, and different values of α.

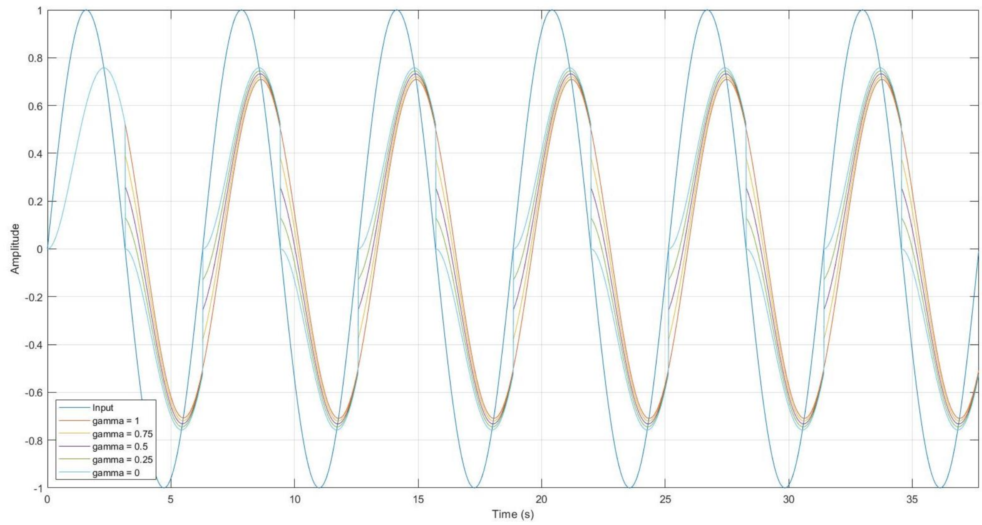

Figure 11. Response of the fractional GFORE to input $e(t) = \sin(t)$, with $\omega_r = 1$, $\alpha = 0.75$, and different values of γ.

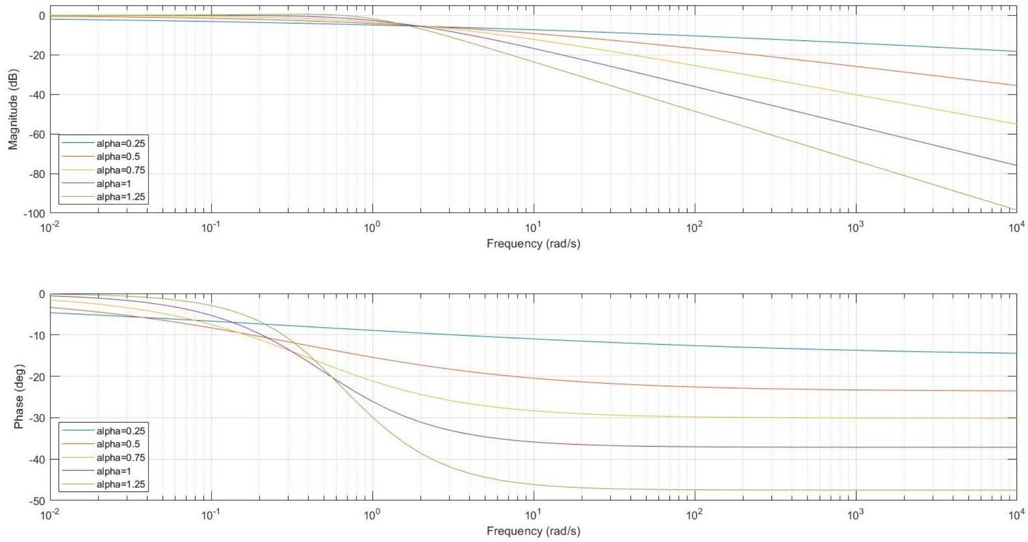

Figure 12. Describing function for the fractional GFORE, with $\omega_r = 1$, and $\gamma = 0$ for several orders of α.

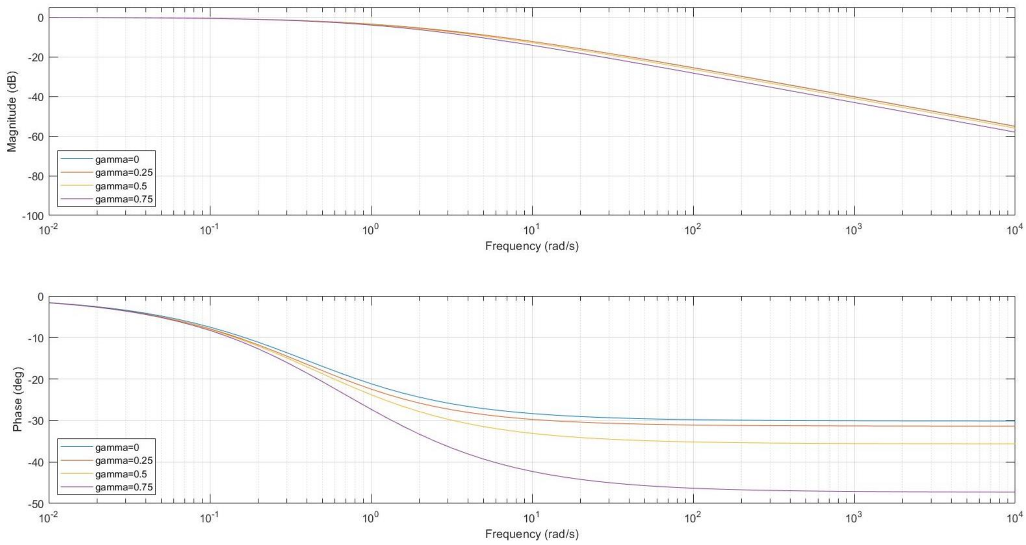

Figure 13. Describing function for the fractional GFORE, with $\omega_r = 1$, and $\alpha = 0.75$ for several orders of γ.

3.4. Other Generalizations

For the fractional generalizations of GSORE, CgLp-GFORE, and CgLp-GSORE, the same rationale was used.

The transfer functions of each are:

1. fractional GSORE

$$G_c = \frac{\omega_r^2}{s^{2\alpha} + 2\beta_r\omega_r s^\alpha + \omega_r^2}, \gamma \tag{23}$$

2. fractional CgLp-GFORE

$$G_c = \frac{\omega_f \omega_{r\eta}}{\omega_r} \frac{s^\alpha + \omega_r}{(s^\alpha + \omega_{r\eta})^{\gamma}(s^\alpha + \omega_f)}, \tag{24}$$

3. fractional CgLp-GSORE

$$G_c = \frac{\omega_f^2 \omega_{r\eta}^2}{\omega_r^2} \frac{s^{2\alpha} + 2\beta_r \omega_r s + \omega_r^2}{(s^\alpha + \omega_f)^2 (s^{2\alpha} + 2\beta_r \omega_{r\eta} s + \omega_{r\eta}^2)} \gamma \tag{25}$$

The equations for the integrable slopes of the states for the fractional controllers are:

1. fractional GSORE

$$D^1 x_{r_2}(t) = D^{1-\alpha}(\omega_r^2 e(t) - \omega_r^2 x_{r_1}(t) - 2\beta_r \omega_r x_{r_2}(t)), \tag{26}$$

$$D^1 x_{r_1}(t) = D^{1-\alpha}(x_{r_2}(t)), \tag{27}$$

2. fractional CgLp-GFORE

$$D^1 x_{r_1}(t) = D^{1-\alpha}(-\omega_{r\eta} x_{r_1}(t) + \omega_{r\eta} e(t)), \tag{28}$$

$$D^1 x_{r_2}(t) = D^{1-\alpha}(\omega_f x_{r_1}(t) - \omega_f x_{r_2}(t)), \tag{29}$$

3. fractional CgLp-GSORE

$$D^1 x_{r_1}(t) = D^{1-\alpha} x_{r_2}(t), \tag{30}$$

$$D^1 x_{r_2}(t) = D^{1-\alpha}(-\omega_{r\eta}^2 x_{r_1}(t) - 2\beta_r \omega_{r\eta} x_{r_2}(t) + \omega_{r\eta}^2 e(t)), \tag{31}$$

$$D^1 x_{r_3}(t) = D^{1-\alpha} x_{r_4}(t), \tag{32}$$

$$D^1 x_{r_4}(t) = D^{1-\alpha}(-\omega_f^2 x_{r_3}(t) - 2\omega_f x_{r_4}(t) + x_{r_1}(t)). \tag{33}$$

The following figures depict, for these controllers, the responses to input $e(t) = \sin(t)$ and the describing functions, for different values of parameters α and γ:

1. fractional GSORE: Figures 14 and 15 (responses to a sinusoid), Figures 16 and 17 (describing functions);
2. fractional CgLp-GFORE: Figures 18 and 19 (responses to a sinusoid), Figures 20 and 21 (describing functions);
3. fractional CgLp-GSORE: Figures 22 and 23 (responses to a sinusoid), Figures 24 and 25 (describing functions).

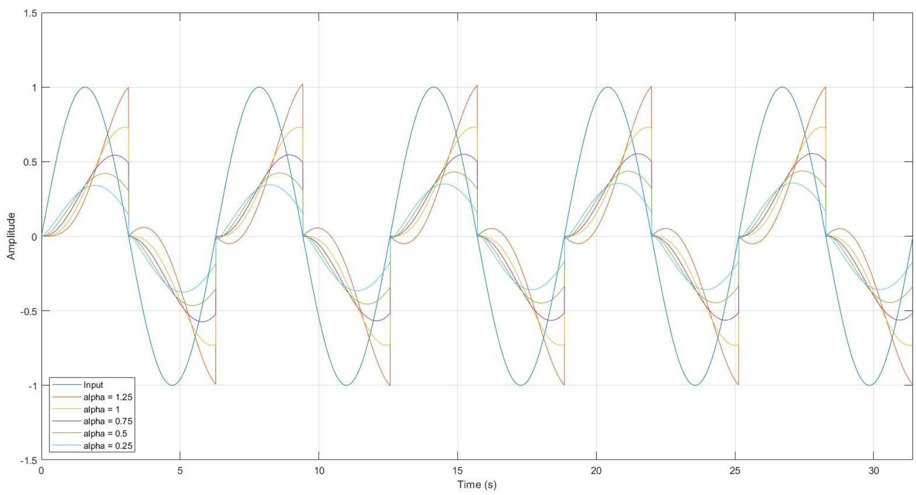

Figure 14. Response of the fractional GSORE to the input $e(t) = \sin(t)$, with $\omega_r = 1$, $\beta = \frac{\sqrt{2}}{2}$, $\gamma = 0$, and different values of α.

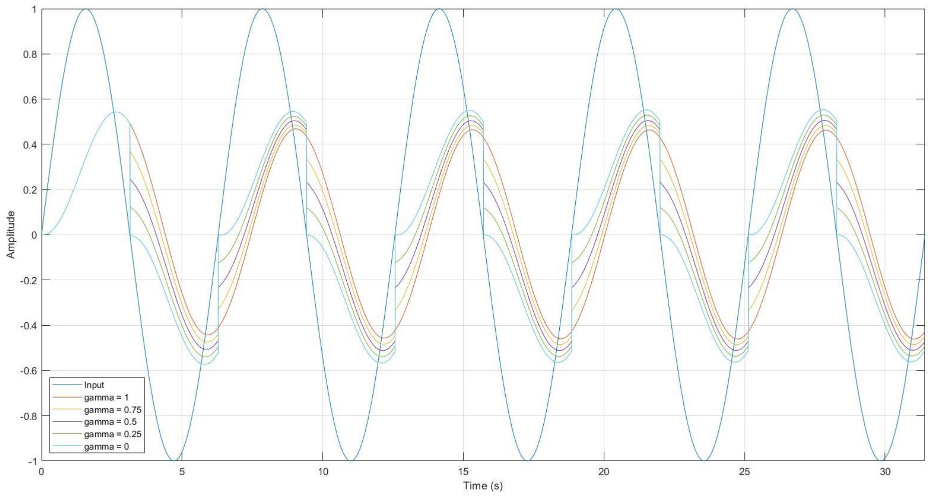

Figure 15. Response of the Fractional GSORE to the input $e(t) = \sin(t)$, with $\omega_r = 1$, $\beta = \frac{\sqrt{2}}{2}$, $\alpha = 0.75$, and different values of γ.

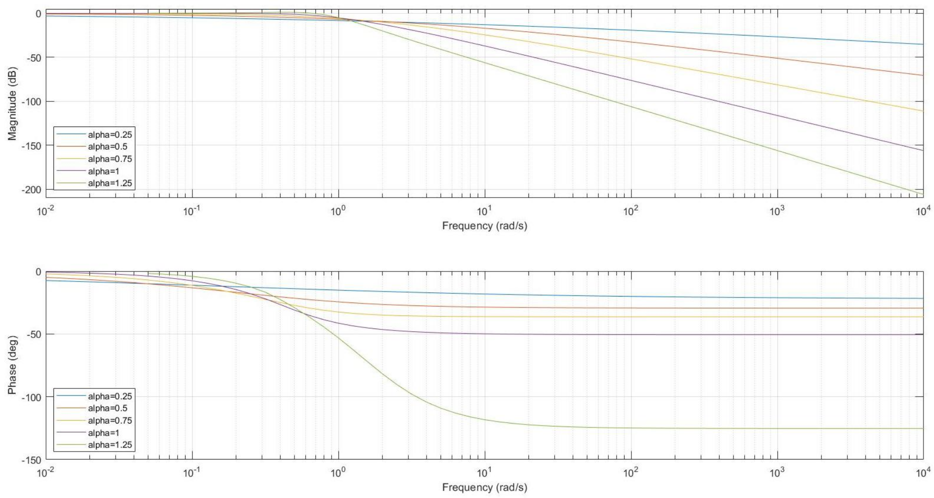

Figure 16. Describing function for the fractional GSORE, with $\omega_r = 1$, $\beta = \frac{\sqrt{2}}{2}$ and $\gamma = 0$ for several orders of α.

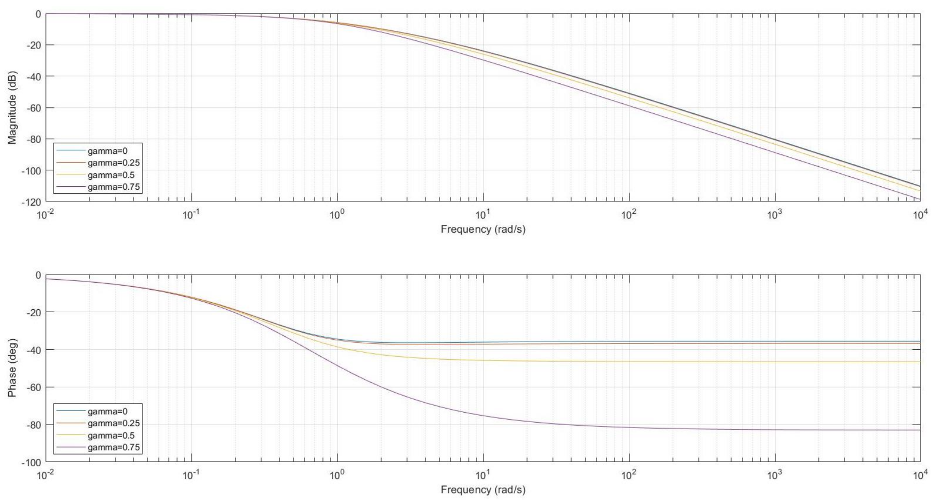

Figure 17. Describing function for the fractional GSORE, with $\omega_r = 1$, $\beta = \frac{\sqrt{2}}{2}$ and $\alpha = 0.75$ for several orders of γ.

3.5. Analysis of the Describing Functions of the Generalizations

Regarding fractional CI, Figure 6 shows how the slopes of the responses seem to be the same before and after the reset. Figure 9 shows that the reduction of the phase lag does not increase proportionally with γ. Figure 8 shows how the gain plots generalize the slope rule to 20α dB/decade.

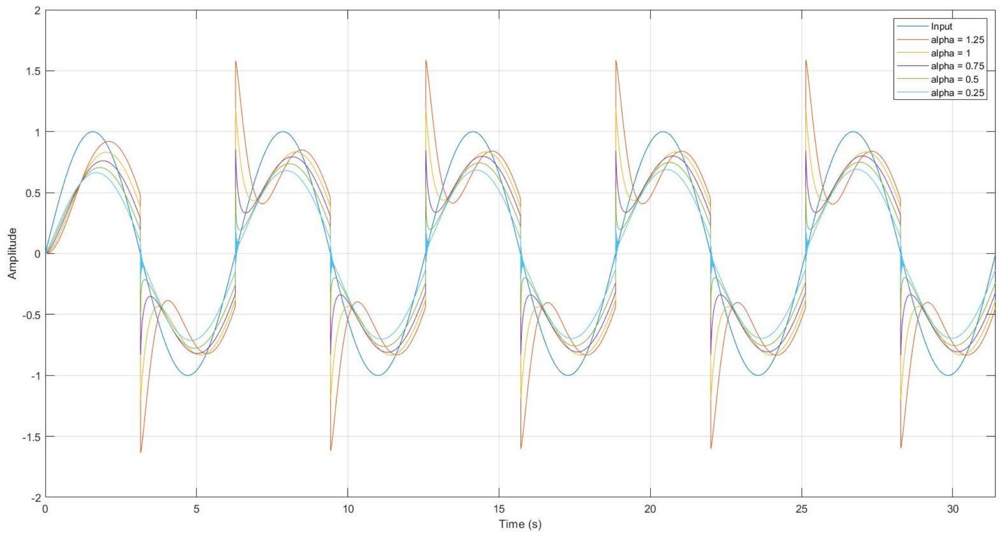

Figure 18. Response of the fractional CgLp-GFORE to the input $e(t) = \sin(t)$, with $\omega_r = 1$, $\omega_\eta = 0.73$, $\omega_f = 3$, $\gamma = 0$, and different values of α.

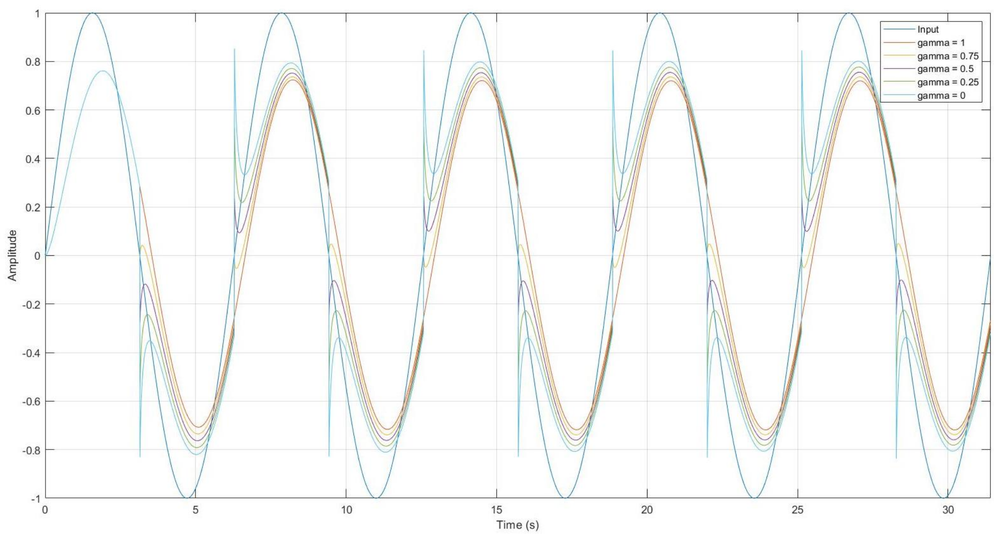

Figure 19. Response of the fractional CgLp-GFORE to the input $e(t) = \sin(t)$, with $\omega_r = 1$, $\omega_\eta = 0.73$, $\omega_f = 3$, $\alpha = 0.75$, and different values of γ.

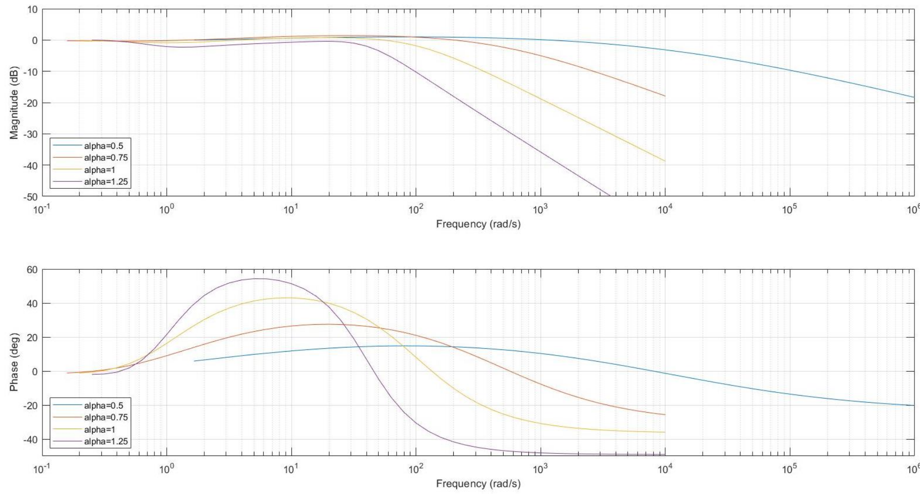

Figure 20. Describing function for the fractional CgLp-GFORE, with $\omega_r = 1$, $\omega_f = 100$, $\omega_{r\eta} = 0.73$ and $\gamma = 0$ for several orders of α.

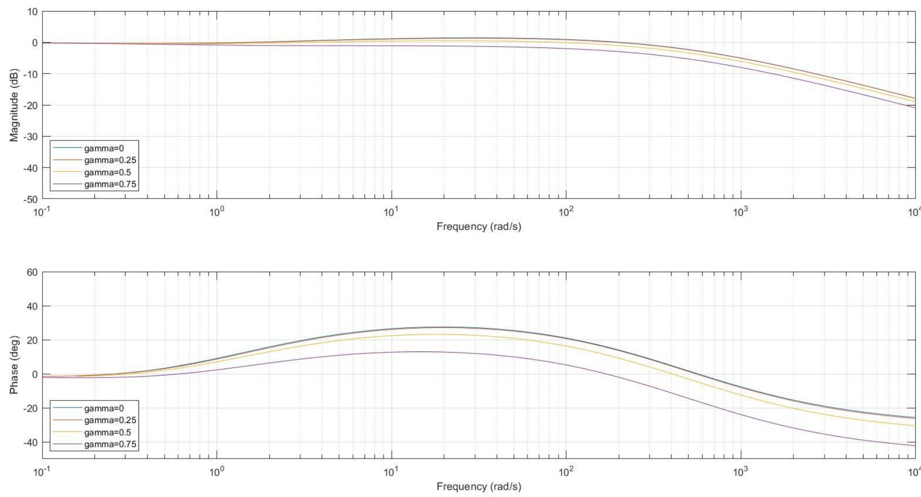

Figure 21. Describing function for the fractional CgLp-GFORE, with $\omega_r = 1$, $\omega_f = 100$, $\omega_{r\eta} = 0.73$ and $\alpha = 0.75$ for several orders of γ.

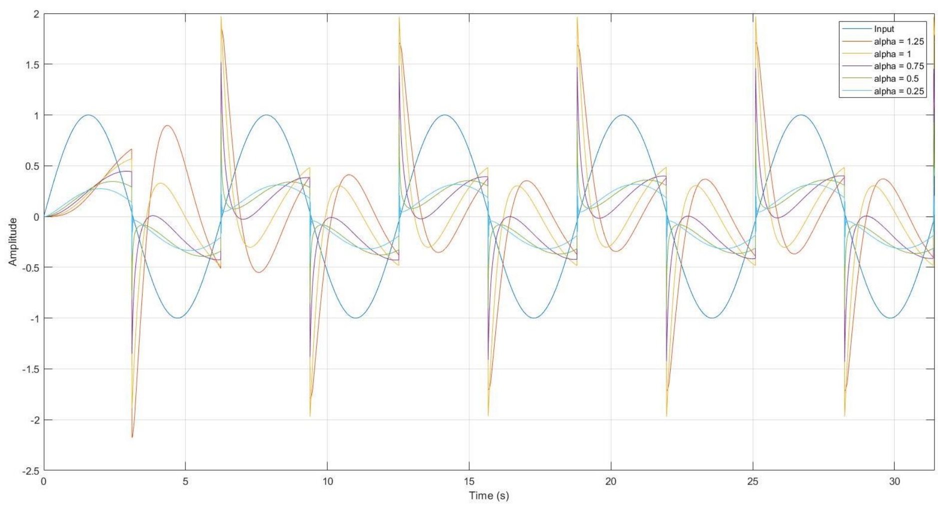

Figure 22. Response of the fractional CgLp-GSORE to the input $e(t) = \sin(t)$, with $\omega_r = 1$, $\omega_\eta = 0.7$, $\omega_f = 1.5$, $\gamma = 0$, and different values of α.

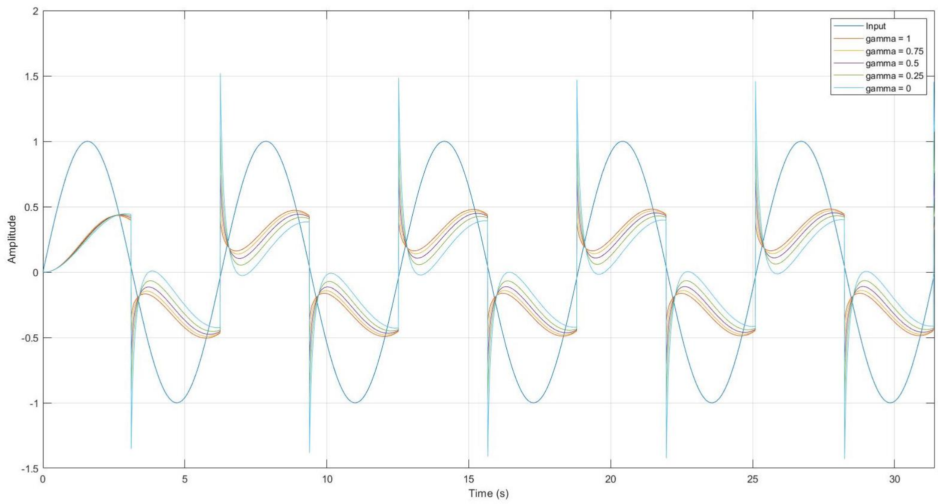

Figure 23. Response of the fractional CgLp-GSORE to the input $e(t) = \sin(t)$, with $\omega_r = 1$, $\omega_\eta = 0.7$, $\omega_f = 1.5$, $\beta = \frac{\sqrt{2}}{2}$, $\alpha = 0.75$, and different values of γ.

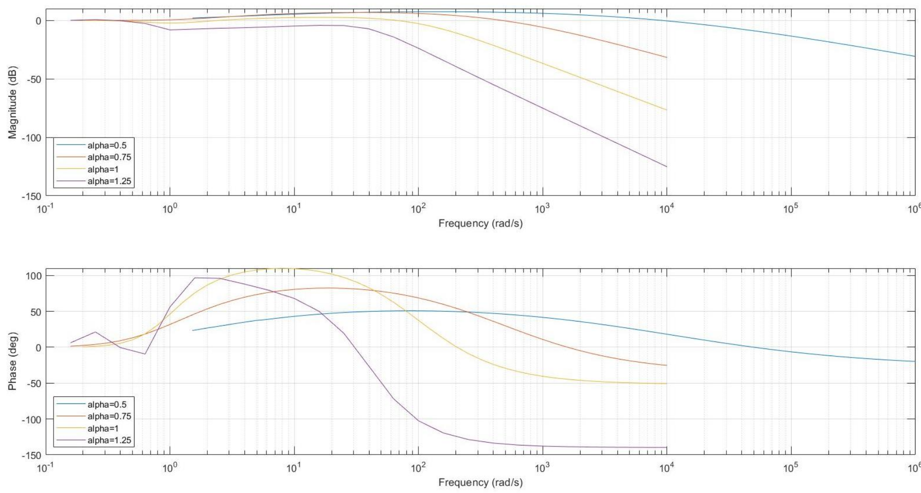

Figure 24. Describing function for the fractional CgLp-GSORE, with $\omega_r = 1$, $\omega_f = 100$, $\omega_{r\eta} = 0.95$, $\beta = \frac{\sqrt{2}}{2}$, and $\gamma = 0$ for several orders of α.

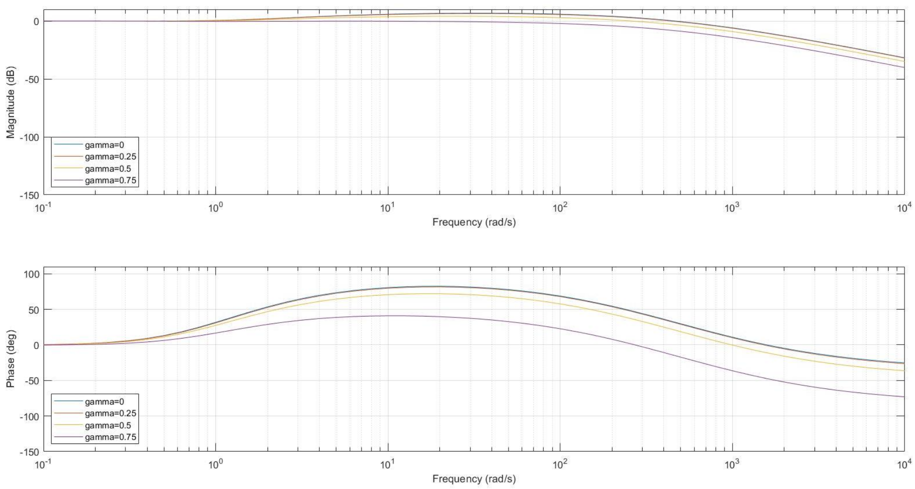

Figure 25. Describing function for the fractional CgLp-GSORE, with $\omega_r = 1$, $\omega_f = 100$, $\omega_{r\eta} = 0.95$, and $\alpha = 0.75$ for several orders of γ.

As for GFrORE, in Figure 12 it is possible to see that the transition band of frequencies around the corner frequency widens significantly with the lowering of α.

Concerning fractional GSORE, one can see in Figure 16 that the decrease in the phase between $\alpha = 1$ and $\alpha = 1.25$ is much more significant than between other orders.

Regarding fractional CgLp-GFORE, Figure 18 shows that the lower orders of α may lead to a less strong kick in the response after reset instances, while Figure 19 shows that low values of γ may have the opposite effect. In Figure 20, it is interesting to see how the bandwidth of the phase lead broadens with the lowering of α at the same time that the phase lead decreases.

Finally, for the fractional CgLp-GSORE, the response of the fractional CgLp-GSORE very easily reaches a significant overshoot, as can be seen in Figures 22 and 23, unless its parameters are carefully tuned to avoid this.

3.6. Application Example

As a final test of the developed implementation of these controllers, a closed-loop system was simulated in MATLAB with a plant $G_p(s)$ to be controlled and its respective controller. The plant in the test was

$$G_P = \frac{40}{s^2 + 2s}, \tag{34}$$

and the following lead compensator was used as the reference integer linear controller:

$$G_{LC} = \frac{4.17s + 18.38}{s + 18.38}. \tag{35}$$

A fractional CgLp-GFORE was subsequently tuned, and the following parameters were achieved:

$$\alpha = 0.88, \quad \gamma = -0.5, \quad \omega_r = 1, \quad \omega_{r\eta} = 0.08, \quad \omega_f = 106,$$

$$K = 15.5, \quad tol = 0.05. \tag{36}$$

The parameters of this fractional CgLp-GFORE were made to adapt twice when $e(t)$ was very close to zero. These changes were $K = 13.9$ and $\gamma = -0.6$, at $t = 0.32$ s, and $K = 14.3$ and $\gamma = -0.6$, at $t = 1$ s.

The comparison of the responses of the closed-loop systems with each of the two controllers to a unit step input can be observed in Figure 26.

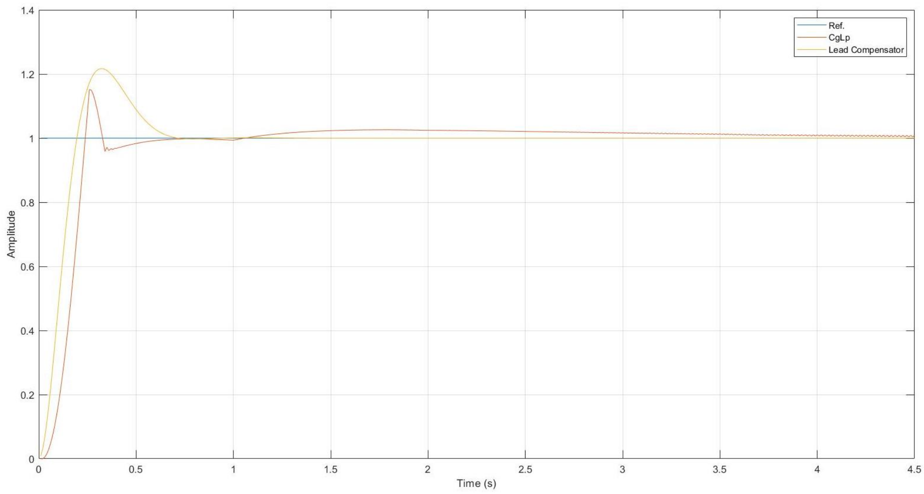

Figure 26. Step responses of the closed-loop systems with controllers *LC* and fractional *CgLp-GFORE* with the specified parameters.

The fractional CgLp achieved a faster response with less overshoot than the linear lead compensator. However, there was a small jump that very slightly deviated from the response from the reference for a short time and tuning required a lot of effort and some unorthodox changes in the parameters. It could be of interest to try and establish a tuning procedure in the future.

4. Conclusions

The present paper presented a general numerical implementation of a fractional reset for controllers, directly through the Grünwald–Letnikov definition, without the need of resorting to any integer order approximation (such as the CRONE approximation).

Reset controllers CI, GFORE, GSORE, CgLp-GFORE, and CgLp-GSORE were implemented and generalized to fractional orders through the previously mentioned fractional reset mechanism. The describing function method was used to assess whether these controllers behaved in the desired fashion, and the achieved result was significantly positive.

Following the work here presented, it is possible to go forward in the following ways:

First, further study into the frequency behaviors of these fractional reset controllers could be carried out. More functions could be computed to better understand the interactions between parameters in CgLp, such as the effect of order α in the corner frequency shift between ω_r and $w_{r\eta}$, or what particular effects the negative values of γ may have.

Another parameter that could be worth analyzing is the tolerance under which the reset takes place. This tolerance may easily change the results, and its adequate value is highly dependent on the sampling time and specific input data. It could be beneficial to find a systematic way to define this tolerance or conceive another method of establishing the instances at which the reset happens.

Regarding the time response of the controllers, fine results can be achieved, but the tuning of parameters may be daunting. A more systematic tuning procedure could be pursued to exploit the full potential of the elements. Moreover, for longer periods of time, the response of the controller takes a long time to compute, since the Grünwald–Letnikov definition makes use of all previous instances for every step, assigning them different weights. Ways to avoid this slowing down could be investigated (for example, in the form of loss of memory [10,19]).

An extensive stability analysis of these merged control methods is a critical step to furthering their study.

Author Contributions: Conceptualization, D.V.; methodology, D.V.; software, H.P.; validation, H.P. and D.V.; formal analysis, H.P. and D.V.; investigation, H.P.; writing—original draft preparation, H.P.; writing—review and editing, D.V.; visualization, H.P.; supervision, D.V.; funding acquisition, D.V. All authors have read and agreed to the published version of the manuscript.

Funding: This work was supported by FCT, through IDMEC, under LAETA, project UIDB/50022/2020.

Institutional Review Board Statement: Not applicable.

Informed Consent Statement: Not applicable.

Data Availability Statement: Not applicable.

Conflicts of Interest: The authors declare no conflict of interest.

References

1. Åström, K.J. Limitations on Control System Performance. *Eur. J. Control* **2000**, *6*, 2–20. [CrossRef]
2. Goodwin, G.C.; Graebe, S.F.; Salgado, M.E. *Control System Design*; Prentice-Hall: Upper Saddle River, NJ, USA; New Delhi, India , 2001.
3. Seron, M.M.; Braslavsky, J.H.; Goodwin, G.C. *Fundamental Limitations in Filtering and Control*; Springer: Berlin/Heidelberg, Germany, 1997 .
4. Beker, O.; Hollot, C.V.; Chait, Y. Plant with integrator: An example of reset control overcoming limitations of linear feedback. In Proceedings of the 2001 American Control Conference, Arlington, VA, USA, 25–27 June 2001.

5. Åström, K.J.; Murray, R.M. *Feedback Systems: An Introduction for Scientists and Engineers*; Princeton University Press: Princeton, NJ, USA, 2008.
6. Clegg, J.C. A nonlinear integrator for Servomechanisms. *Trans. Am. Inst. Electr. Eng. Part II Appl. Ind.* **1958**, *77*, 41–42. [CrossRef]
7. Guo, Y.; Wang, Y.; Xie, L. Frequency-domain properties of reset systems with application in hard-disk-drive systems. *IEEE Trans. Control Syst. Technol.* **2009**, *17*, 1446–1453.
8. Hazeleger, L.; Heertjes, M.; Nijmeijer, H. Second-order reset elements for Stage Control Design. In Proceedings of the 2006 American Control Conference (ACC), Minneapolis, MN, USA, 14–16 June 2006.
9. Saikumar, N.; Sinha, R.K.; HosseinNia, S.H. "Constant in gain lead in phase" element—Application in Precision Motion Control. *IEEE/ASME Trans. Mechatron.* **2019**, *24*, 1176–1185. [CrossRef]
10. Valério, D.; Sá da Costa, J. *An Introduction to Fractional Control*; IET Control Engineering Series, 91; Institution of Engineering and Technology: London, UK, 2013.
11. Valério, D.; Sá da Costa, J. Fractional reset control. *Signal Image Video Process.* **2012**, *6*, 495–501. [CrossRef]
12. HosseinNia, S.H.; Tejado, I.; Vinagre, B.M. Fractional-order Reset Control: Application to a servomotor. *Mechatronics* **2013**, *23*, 781–788. [CrossRef]
13. Monje Concepción, A. *Fractional-Order Systems and Controls: Fundamentals and Applications*; Springer: Berlin/Heidelberg, Germany, 2010.
14. Saikumar, N.; HosseinNia, H. Generalized Fractional Order Reset Element (GFrORE). In Proceedings of the 9th European Nonlinear Dynamics Conference, Budapest, Hungary, 21–30 June 2017.
15. Chen, L.; Saikumar, N.; HosseinNia, S. Development of Robust Fractional-Order Reset Control. *IEEE Trans. Control Syst. Technol.* **2020**, *28*, 1404–1417. [CrossRef]
16. Karbasizadeh, N.; Saikumar, N.; HosseinNia, S. Fractional-order single state reset element. *Nonlinear Dyn.* **2021**, *104*, 413–427. [CrossRef]
17. Oustaloup, A.; Mathieu, B.; Melchior, P.L. *Commande CRONE: Commande Robuste d'Ordre Non Entier*; Hermès: Paris, France, 1991.
18. Valério, D.; Ortigueira, M.D.; Lopes, A.M. How Many Fractional Derivatives Are There? *Mathematics* **2022**, *10*, 737. [CrossRef]
19. Podlubny, I. *Fractional Differential Equations*; Academic Press: San Diego, CA, USA, 1999.
20. Miller, K.; Ross, B.A. *Introduction to the Fractional Calculus and Fractional Differential Equations*; Wiley: New York, NY, USA, 1993.
21. Ortigueira, M.D.; Tenreiro Machado, J.A. What is a fractional derivative? *J. Comput. Phys.* **2015**, *293*, 4–13. [CrossRef]
22. Ortigueira, M.D.; Tenreiro Machado, J. A. Which Derivative? *Fractal Fract.* **2017**, *1*, 3. [CrossRef]
23. Yang, X.; Peng, D.; Lv, X.; Li, X. Recent progress in impulsive control systems. *Math. Comput. Simul.* **2017**, *155*, 244–268. [CrossRef]